

p. 17 delete footnote
2 - 1000 - 17 3p

Sensor and Simulation Notes
Note 99
March 1970
On the Pulse Excitation of a Cylinder in a Parallel
Plate Waveguide

Clayborne D. Taylor
Mississippi State University
State College, Mississippi 39762

and

George A. Steigerwald
Electromagnetic Hazards Division 2627
Sandia Laboratories, Albuquerque

ABSTRACT

This report studies the problem of obtaining the relation between the current induced on the cylinder in the parallel plate environment and that induced in the free space environment.

CLEARED FOR PUBLIC RELEASE

PL-94-1094, 13 Dec 94



Introduction

A perfectly conducting cylinder is placed symmetrically between the plates of a parallel plate waveguide as shown in Figure 1. It is then considered to be illuminated by a Heaviside unit function (also called the unit step function¹) pulse formed by the TEM mode of the waveguide.² The problem studied is that of obtaining the relation between the current that is induced on the cylinder in the parallel plate environment and the current induced in the free space environment (represented by requiring $\delta/L \rightarrow \infty$).

In examining the harmonic current induced on the cylinder, it is found that the resonant frequency of the cylinder is relatively independent of the plate spacing within the accuracy of the numerical results and for $\delta/L > 0.01$. Figure 2 exhibits the effect of the plates on the peak harmonic current at the center of the cylinder for two particular aspect ratios, $L/D = 10$ and $L/D = 100$. The current comparisons are made at essentially the same frequencies for each aspect ratio. Figure 3 exhibits the effect of the plates on the peak harmonic current at the point half the distance from the end of the cylinder to the center.

An appropriate superposition of the harmonic current yields the induced current under transient excitation. For convenience in this study, the transient excitation is considered to be a Heaviside unit function pulse, i. e., the peak electric field is normalized to 1 volt/meter. It is found that the peak current is obtained before interaction with the plates can occur. Hence, the peak currents are expected to be independent of the plate spacing. For the parameters investigated the foregoing is indeed observed.

The steady state scattering of a cylinder in a parallel plate waveguide has been treated in depth in an earlier paper, which is presented in the Appendix. The foregoing is used here to obtain the time-harmonic currents induced on the cylinder. To treat pulse incidence requires the appropriate Fourier superposition of the harmonic currents with the Fourier transform of the incident pulse, e. g., see Reference 3. For convenience, the incident pulse is considered to be in the form of the aforementioned Heaviside unit function.

After the initial excitation, the current on the cylinder oscillates almost sinusoidally at

the resonant frequency with exponential damping (e.g., see Figure 9). This behavior is sometimes referred to as ringing. Investigations of the cylinder within the parallel plate waveguide reveal a strong dependence of the exponential damping on the separation of the plates. Figure 4 exhibits this dependence for two particular aspect ratios. The damping constant α appearing in Figure 4 is defined,

$$\alpha = \frac{1}{\tau} ,$$

where τ is the time in seconds required for the current to be damped $1/e$ of its initial value. This damping, of course, is due to energy loss through radiation.

Table I is included so that peak currents and decay constants may be computed from data presented in Figures 2 through 4 for various cylinder lengths and plate separations. Note that in the data presentation an attempt is made to present the data in a form for maximum utility.

Figures 5 through 12 are included to indicate the accuracy of the previous data and to illustrate the numerical techniques employed. First the harmonic currents were obtained. Figures 5 through 8 show the harmonic currents at the center and half the distance from the center to the cylinder end for two different aspect ratios and for several different δ/L ratios. Figures 9 through 12 are the corresponding time histories.

It should be pointed out that the results for the aspect ratio $L/D = 10$ are strictly valid only for thin-walled cylindrical shells without end caps. Whether or not the results are valid for solid cylinder is suspect. This will be discussed further below.

Analysis

To effect the solution for the harmonic currents (assumed but suppressed time dependence is $e^{j\omega t}$) one must solve the integral equation,

$$\int_{-L/2}^{L/2} du \hat{I}_0(u) \overline{K}(z, u) = C_1 \cos \beta z - j \frac{4\pi E_0}{\zeta_0} . \quad (1)$$

where

$$\bar{K}(z, u) = \sum_{h=-\infty}^{\infty} K[z, u + 2n(L/2 + \delta)] , \quad (2)$$

$$K(z, z') = \frac{\exp\left[-j\beta \sqrt{(z - z')^2 + a^2}\right]}{\sqrt{(z - z')^2 + a^2}} .$$

(Derivation of Eq. (1) is shown in the Appendix). Here the coordinate z locates the position along the axis of the cylinder and is measured from the center of the cylinder. Also $\beta = 2\pi/\lambda$ is the usual propagation constant and $\zeta_0 = \sqrt{\mu_0/\epsilon_0}$ is the wave impedance of the medium within the waveguide, for air $\zeta_0 \simeq 120\pi$ ohms.

The solution of (1) may be obtained as suggested in the Appendix; however, following the suggestion presented in Reference 4 does expedite the technique considerably. In obtaining the data presented in Figures 5 through 8, a piecewise-constant representation with 41 terms is used for the current distribution to solve (1). For the parameters considered, the data presented there are generally within 10% of the exact values, i. e., the exact solution of (1).

However, it should be pointed out that the boundary conditions employed, namely

$$\hat{I}_0(\pm L/2) = 0 ,$$

restrict the cylinder to a perfectly conducting infinitesimally thin cylindrical shell without end caps. But if the cylinder is thin the results should apply as well for cylinders with end caps. On the other hand, the results may not apply to thick cylinders (i. e., $L/D \lesssim 10$) with end caps. Recently it was verified that in a free space region, (1) does yield sufficiently accurate results for engineering purposes if it is applied to thick cylinders with end caps.⁵ Unfortunately, with thick cylinders with end caps in a parallel plate waveguide, (1) may not be sufficient, particularly because of the interaction between the end cap currents and the plates of the waveguide. This question concerning thick cylinders remains to be answered by experimental investigation or an improved theoretical development.

TABLE I

Critical Values for Free Space Current

	<u>L/D = 10</u>	<u>L/D = 100</u>
(BL)res	2.6	3.0
$ \hat{I}_s(0) _{\max}/LE_o$	0.0114 A/V	0.00990 A/V
$ \hat{I}_s(L/4) _{\max}/LE_o$	0.00902 A/V	0.00706 A/V
$\alpha_s L/C$	0.400	0.288
$ \hat{I}_s(0) _{\max}/L$	0.00329 A/m	0.00167 A/m
$ \hat{I}_s(L/4) _{\max}/L$	0.00232 A/m	0.00104 A/m

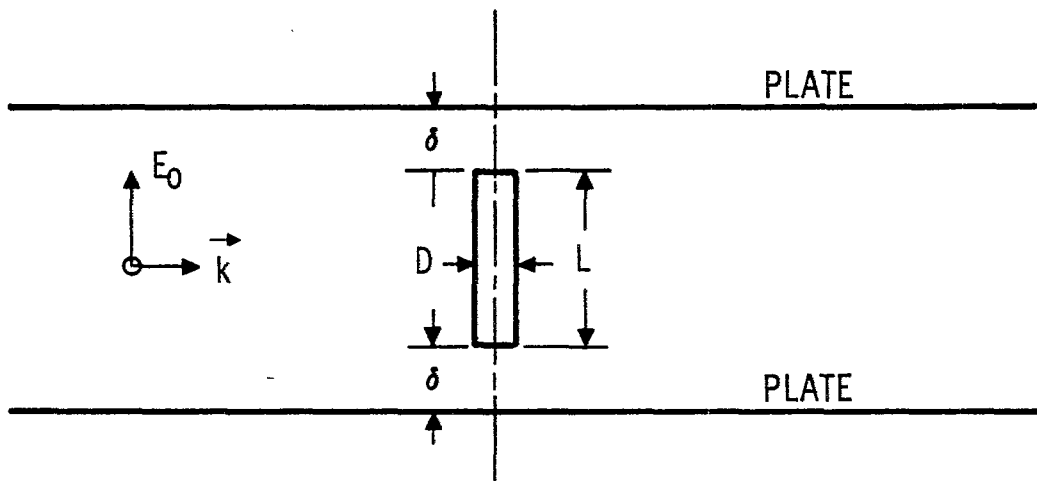


Figure 1. Wire antenna in a parallel plane waveguide. L is the length of the cylinder, D is the diameter, and E_0 is the complex amplitude of the incident electric field.

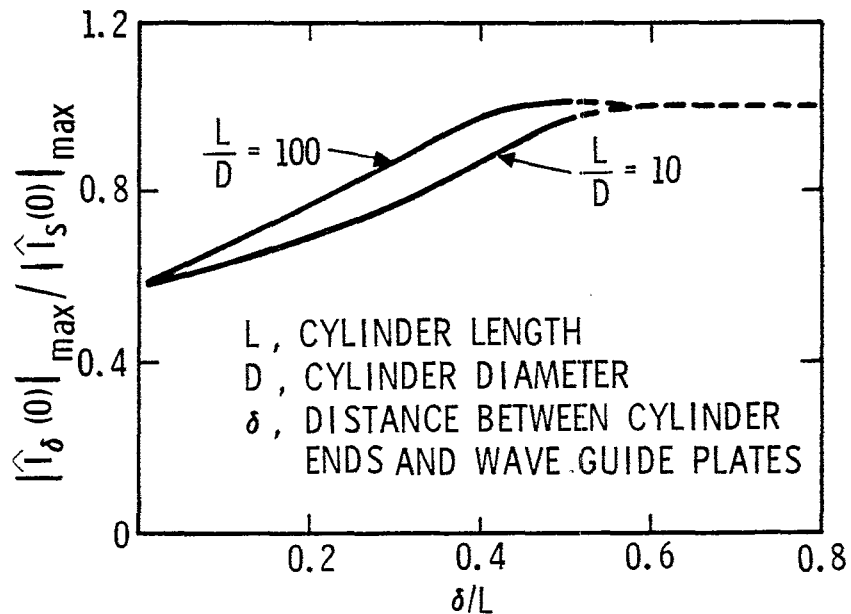


Figure 2. Effect of the plates on the magnitude of the center current. $|\hat{I}_s(0)|_{\max}$ is the maximum harmonic center current in free space and $|\hat{I}_\delta(0)|_{\max}$ is the maximum center current in the parallel plate waveguide.

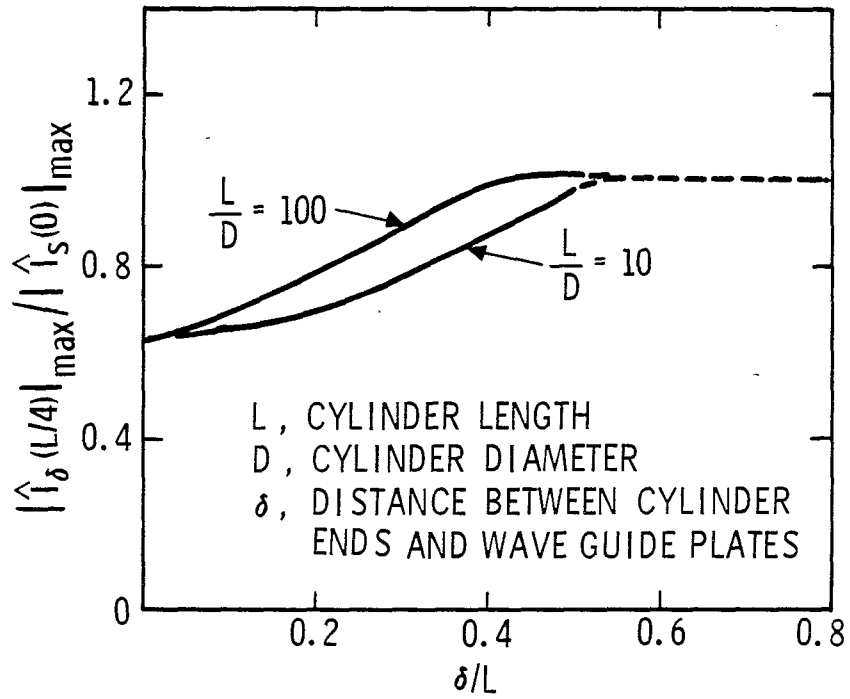


Figure 3. Effect of plates on the magnitude of the maximum current half distance from center to cylinder end.

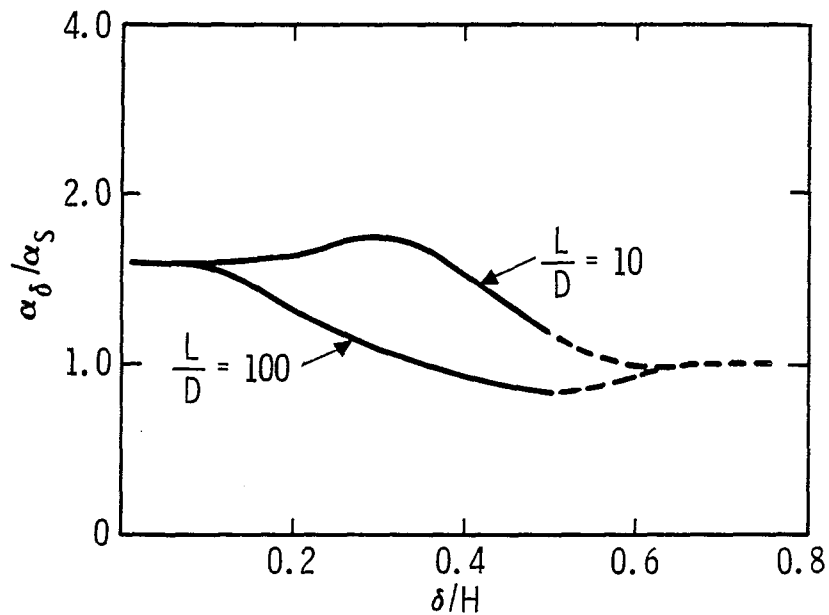


Figure 4. Effect of the plates on the damping constant of the current. α_s is the free space damping constant and α_δ is the damping constant for the cylinder within the parallel plate waveguide.

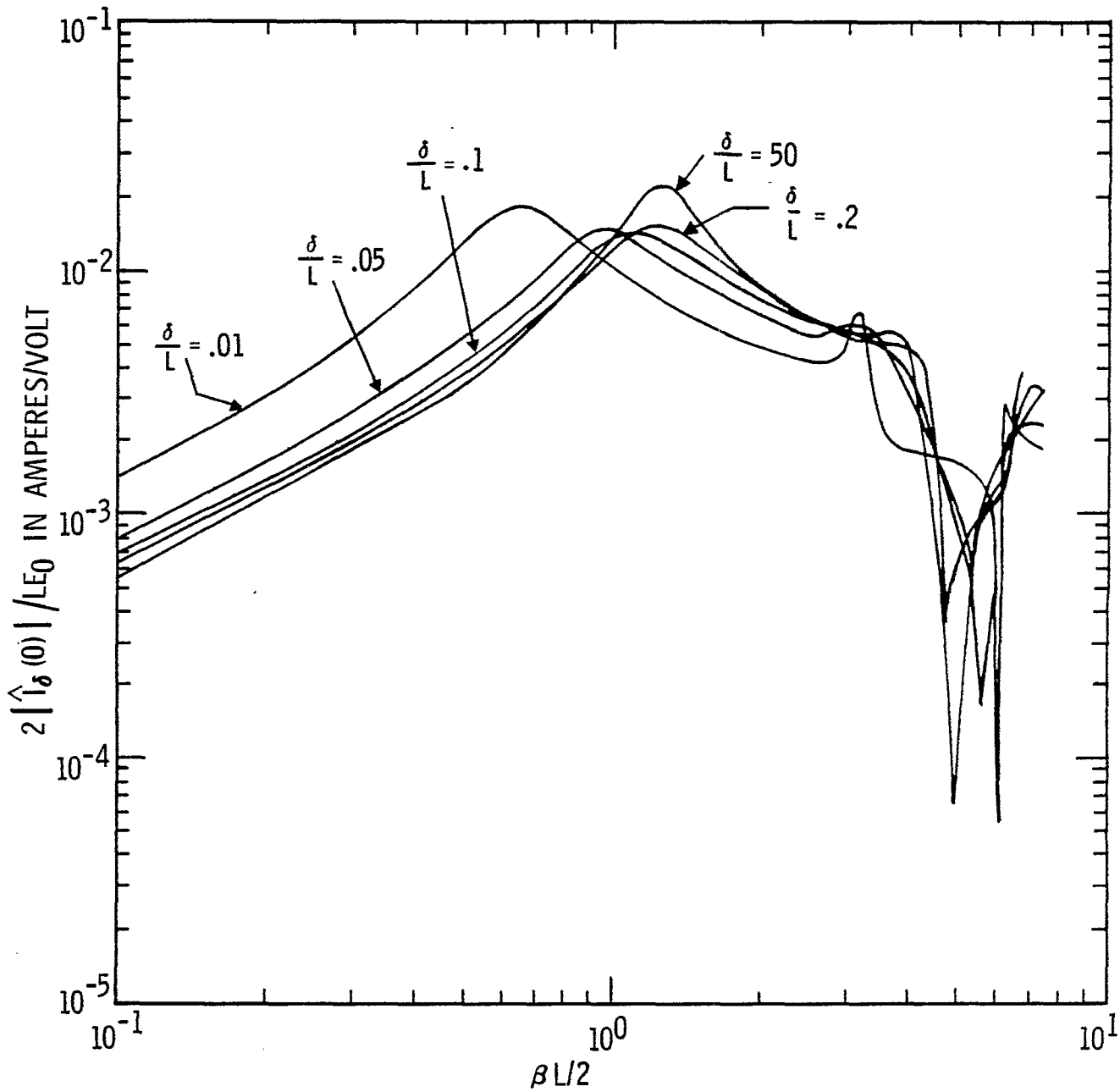


Figure 5. Harmonic center current versus electrical length. Here $L/D = 10$ and $\delta/L = 0.01, 0.05, 0.1, 0.2$ and 50 .

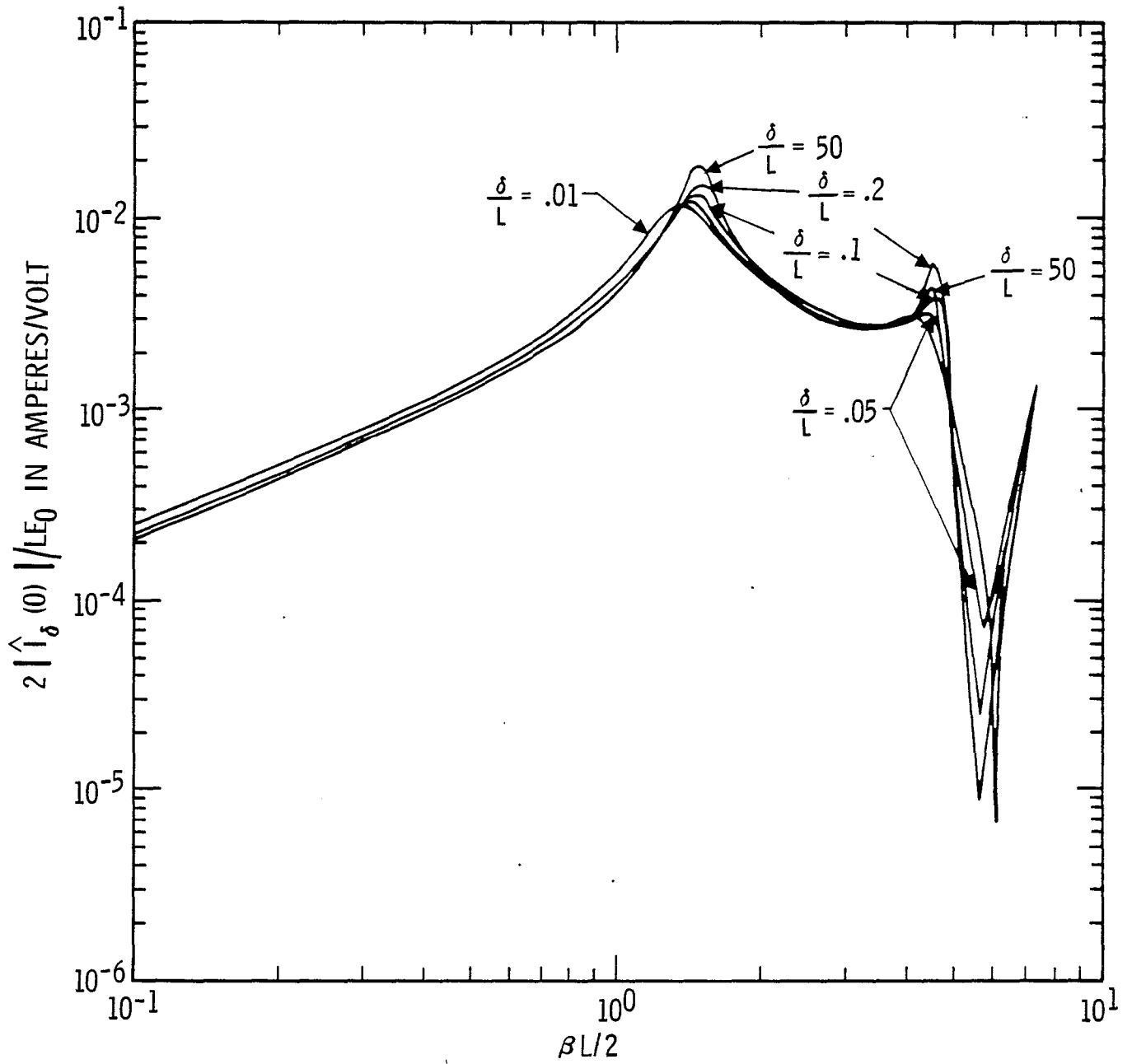


Figure 6. Harmonic center currents versus electrical length.
 Here $L/D = 100$ and $\delta/L = 0.01, 0.05, 0.1, 0.2$ and 50 .

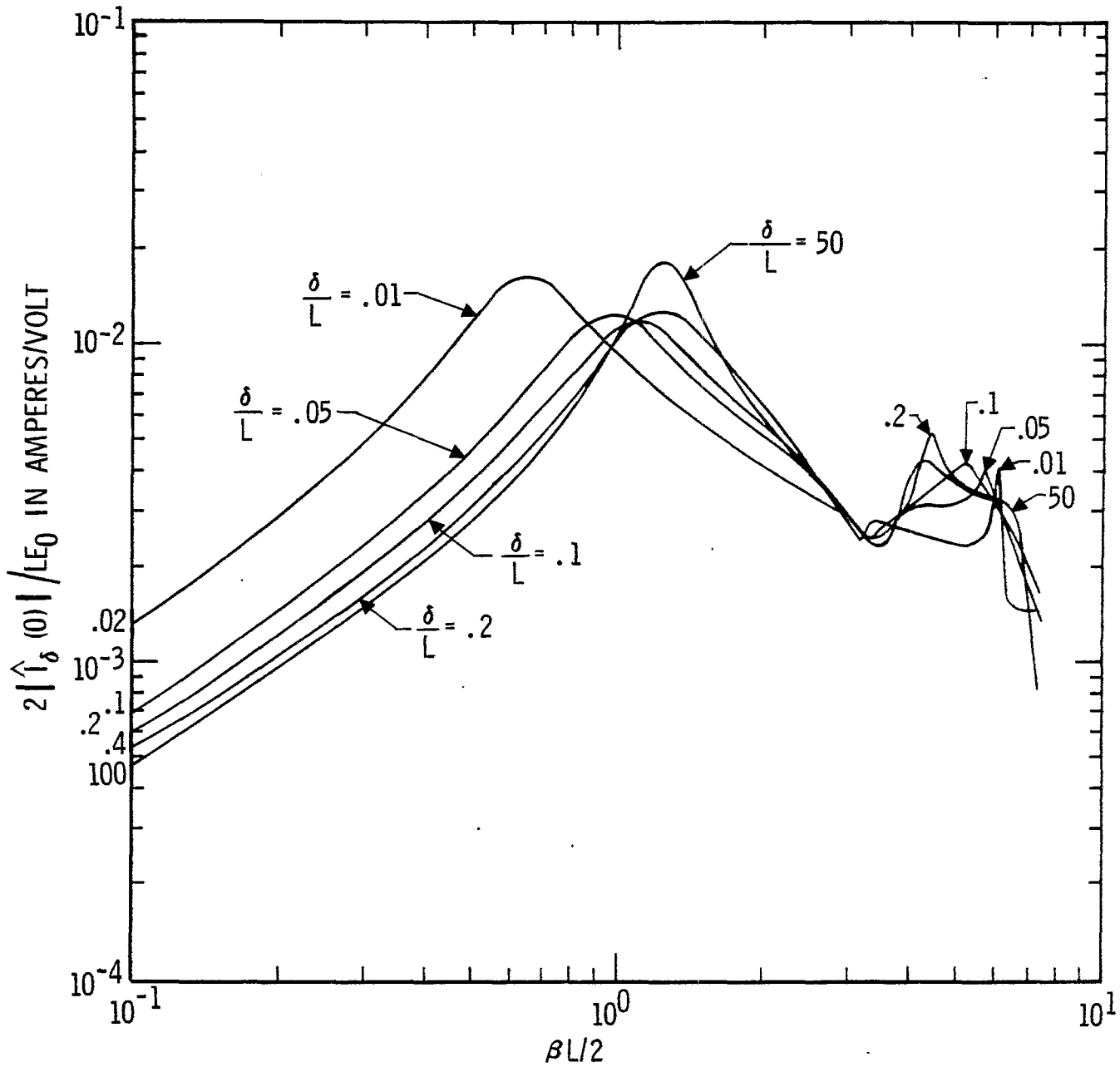


Figure 7. Harmonic currents half distance between center and cylinder end versus electrical length. Here $L/D = 10$ and $\delta/L = 0.01, 0.05, 0.1, 0.2$ and 50 .

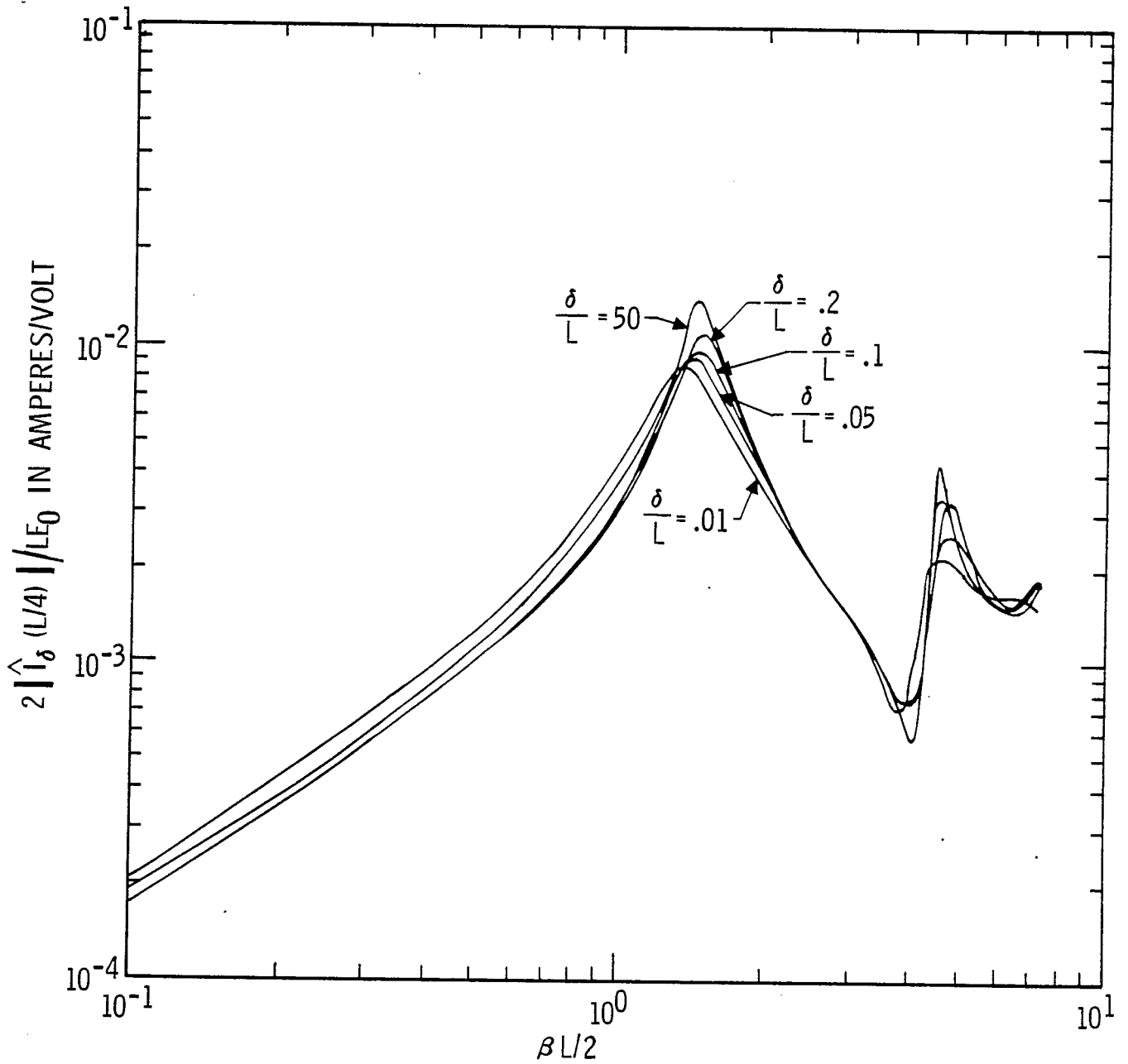


Figure 8. Harmonic currents half distance between center and end versus electrical length. Here $L/D = 100$ and $\delta/L = 0.01, 0.05, 0.1, 0.2$ and 50 .

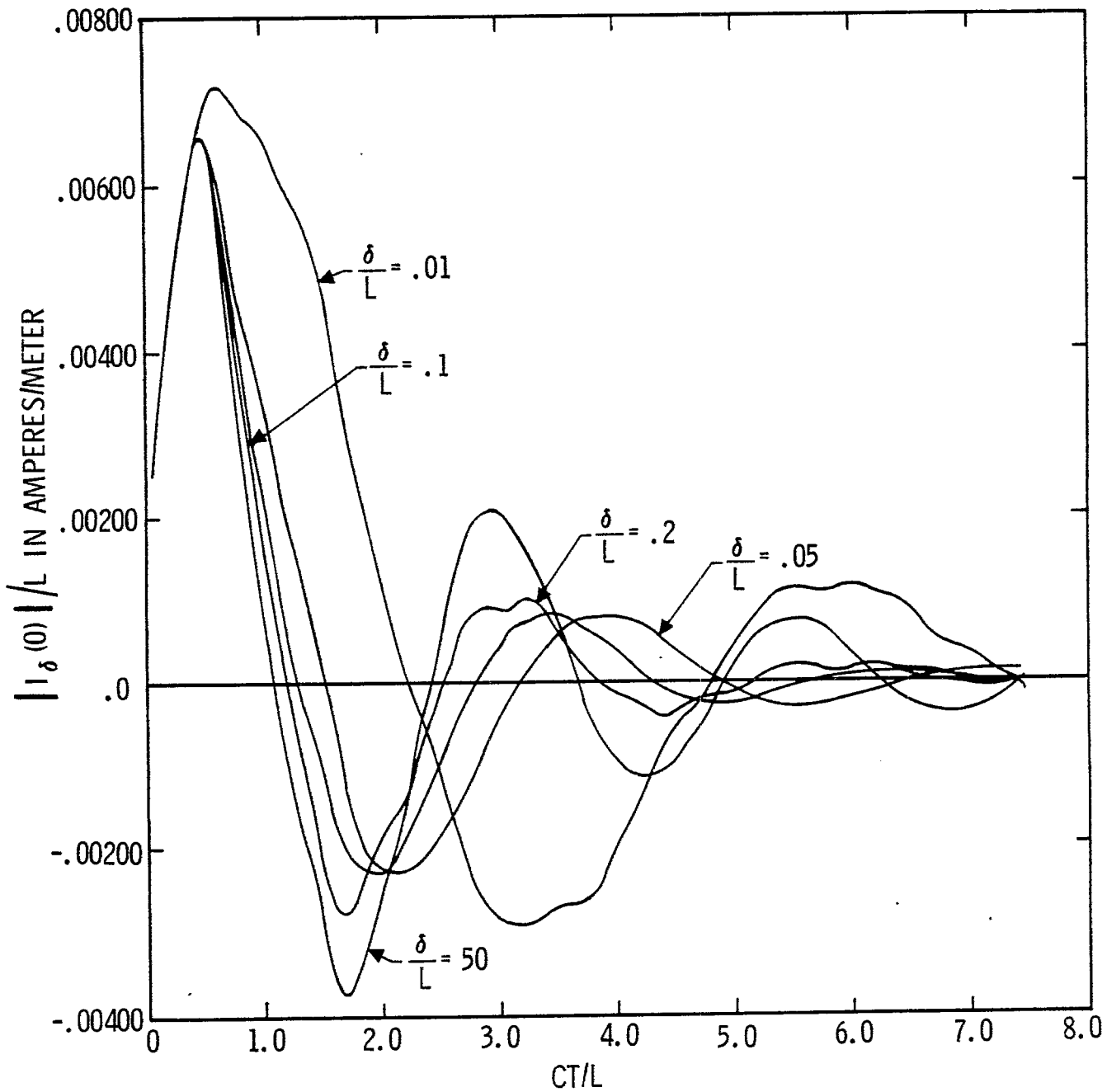


Figure 9. Time histories of the center current for a Heaviside unit function field pulse. Here $L/D = 10$ and $\delta/L = 0.01, 0.05, 0.1, 0.2$ and 50 .

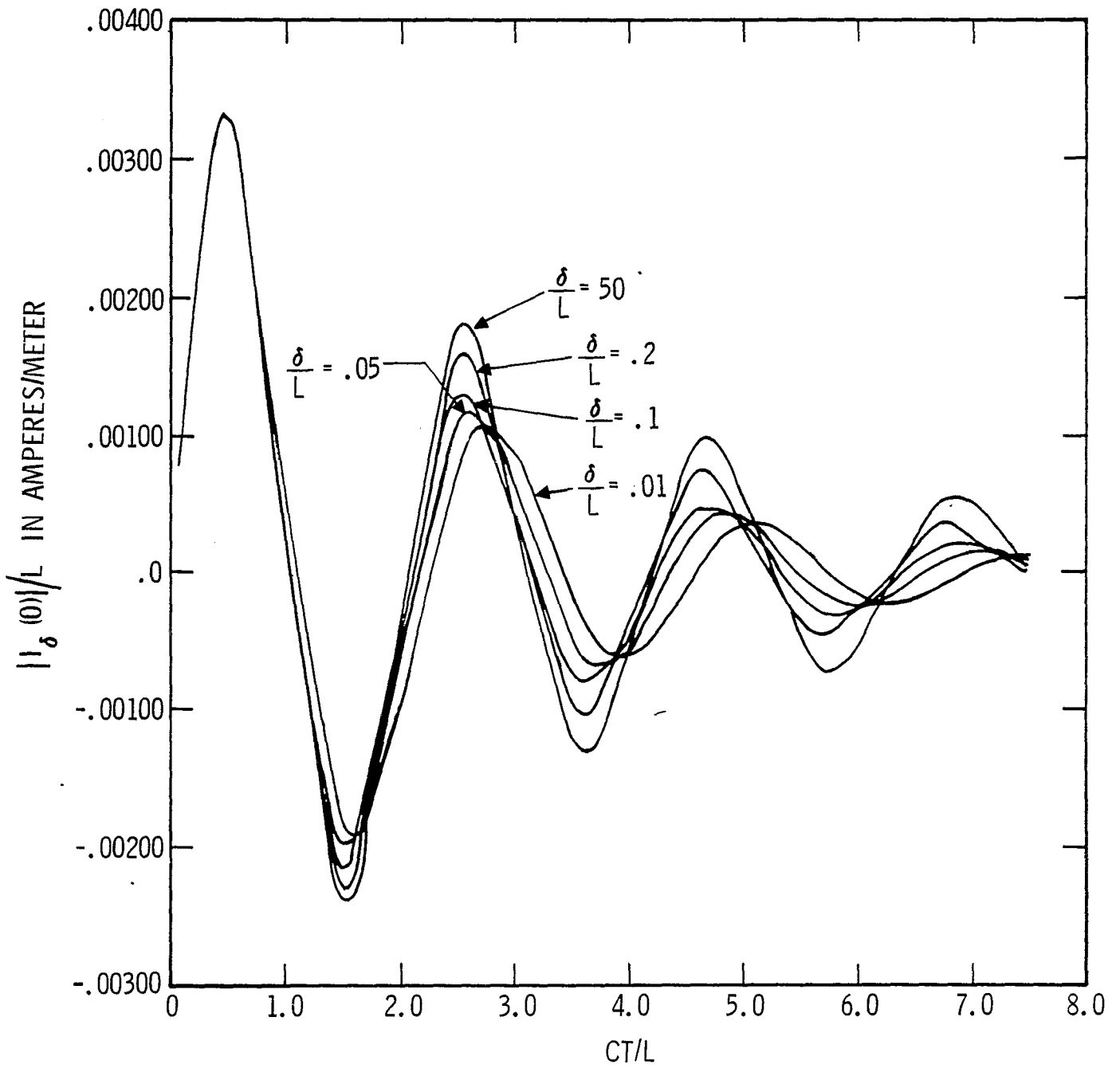


Figure 10. Time histories of the center current for a Heaviside unit function field pulse. Here $L/D = 100$ and $\delta/L = 0.01, 0.05, 0.1, 0.2$ and 50 .

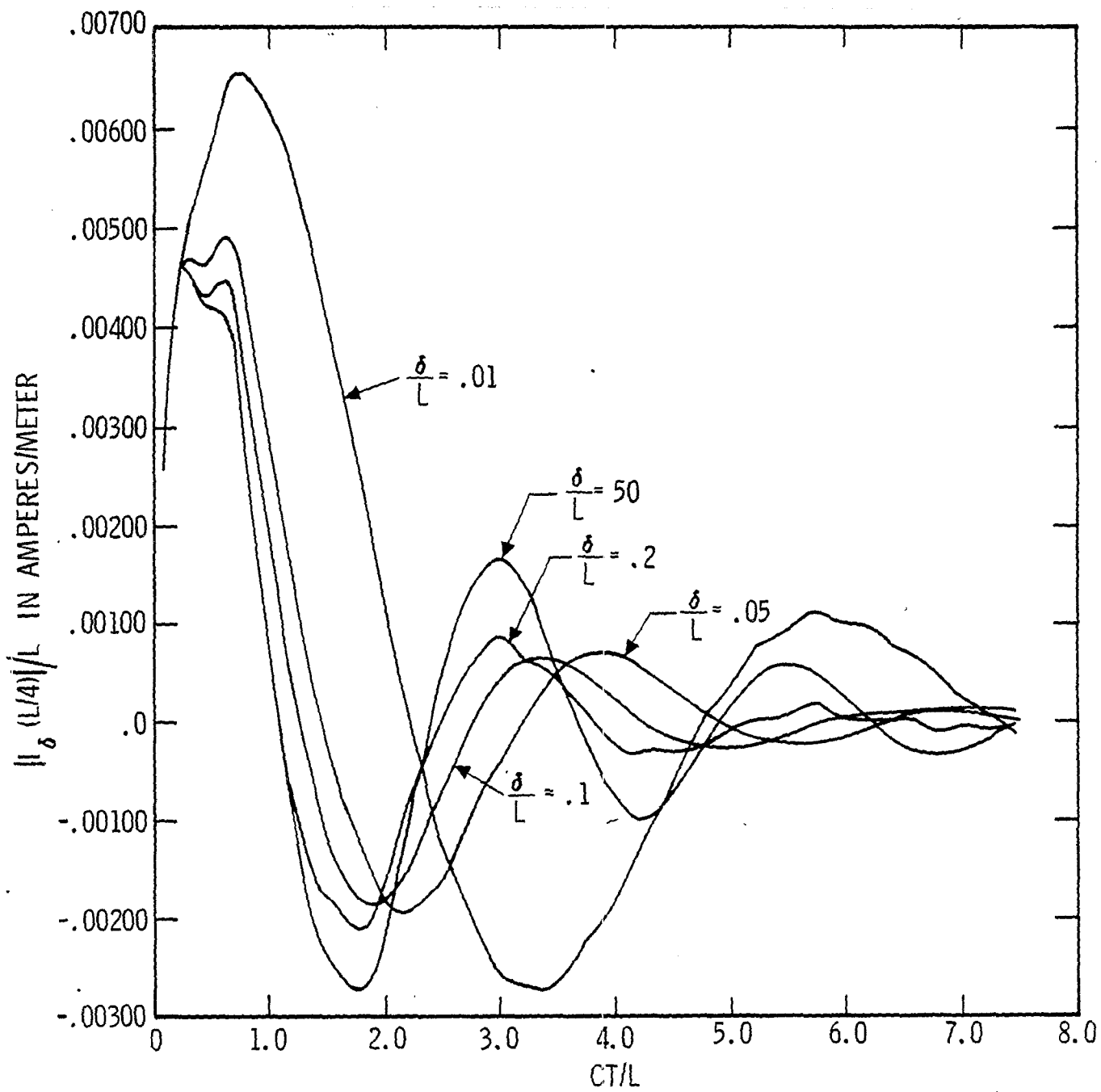


Figure 11. Time histories of currents half distance between center and end for a Heaviside unit function field pulse. Here $L/D = 10$ and $\delta/L = 0.01, 0.05, 0.1, 0.2$ and 50 .

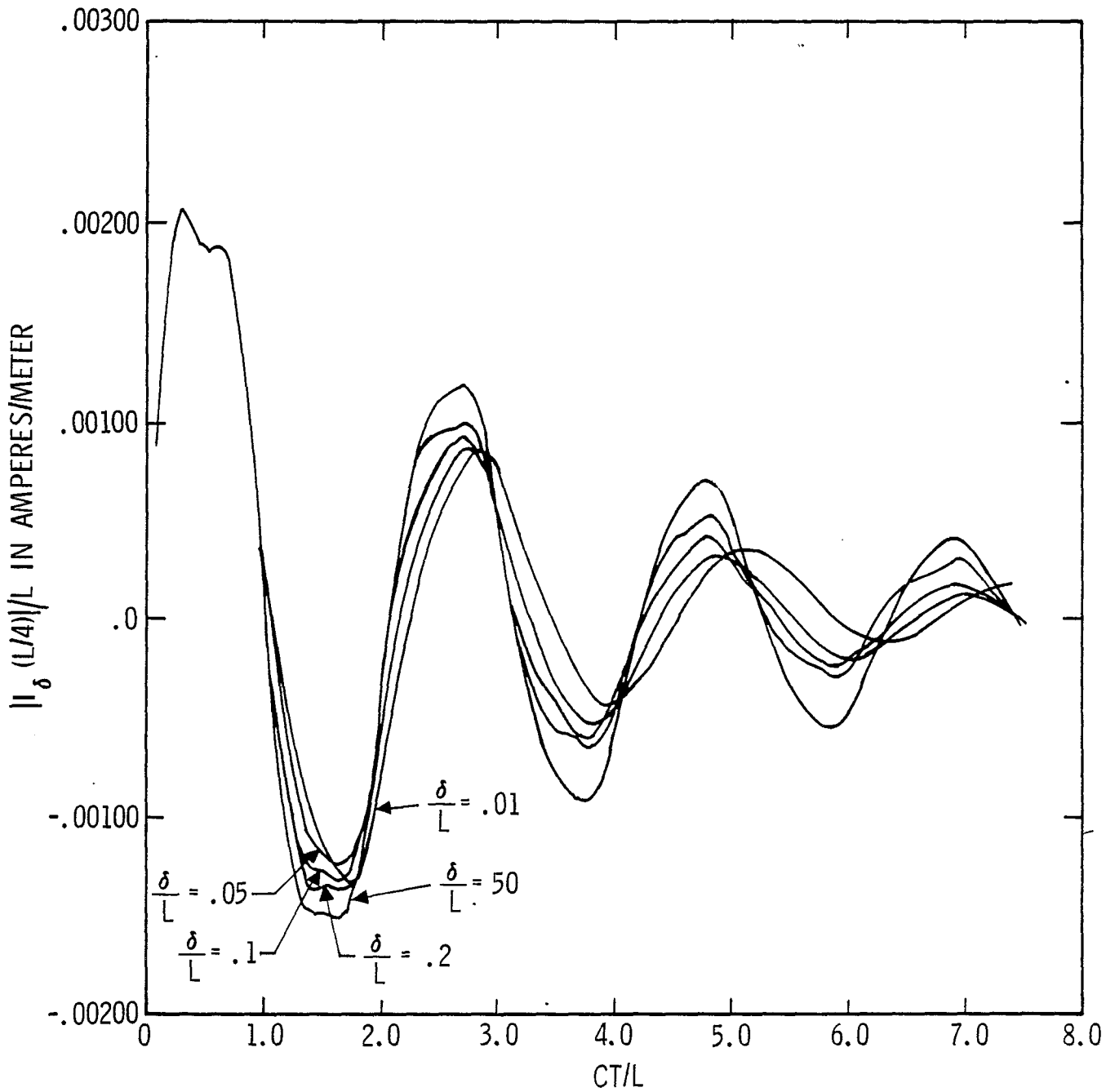


Figure 12. Time histories of currents half distance between center and end for a Heaviside unit function field pulse. Here $L/D = 100$ and $\delta/L = 0.01, 0.05, 0.1, 0.2$ and 50 .

REFERENCES

1. Max Born and Emil Wolf, Principles of Optics, 3rd Ed., p. 757, Pergamon Press, New York, 1965.
2. D. S. Jones, Theory of Electromagnetism, Section 5.5, Pergamon Press, New York, 1964.
3. C. D. Taylor and T. H. Shumpert, "Electromagnetic Pulse Generation by an Impedance Loaded Dipole Antenna," to appear in the January 1970 issue of IEEE Trans. Ant. Prop.
4. E. A. Aronson and C. D. Taylor, "Matrix Methods for Solving Antenna Problems," IEEE Trans. Ant. Prop., AP-15, No. 2, 696-697, September 1967.
5. C. D. Taylor, "On the Exact Theory of a Prolate Spheroidal Receiving and Scattering Antenna," Radio Sci., Vol. 2, No. 3, 351-360, March 1967.

APPENDIX

THIN WIRE RECEIVING ANTENNA IN A PARALLEL PLATE WAVEGUIDE*

In certain experimental antenna studies, very large field strengths are required. To generate these fields in free space requires an exorbitant amount of power. Thus, a waveguide configuration is suggested; in particular, a parallel plate waveguide. However, there is then a question as to how the receiving properties of the antenna in the parallel plate region differ from the antenna in free space.

Consider a parallel plate waveguide with a thin wire antenna located between the plates such that the axis of the antenna is perpendicular to the plates and the midpoint of the antenna is located midway between the plates. Further, it is considered for convenience that only the fundamental waveguide mode is propagating in the waveguide region and incident upon the antenna. This configuration is shown in Figure A1. It is most convenient to apply the use of images to solve this boundary value problem. Because of having two plates, there is an infinite array of colinear images, equidistant apart, both above and below the thin wire antenna (see Figure A1).

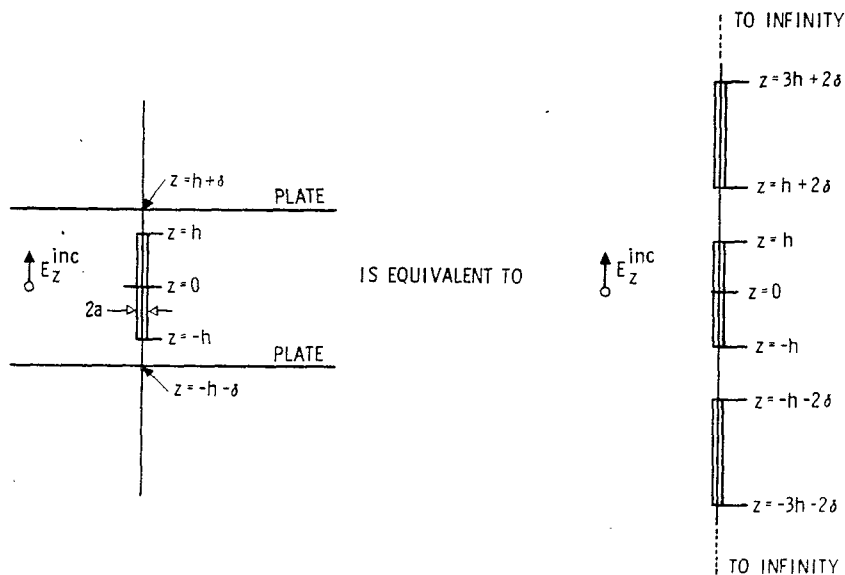


Figure A-1. A thin wire antenna in a parallel plate waveguide with ten equivalent colinear image configurations.

*Taken from the IEEE Transactions on Antennas and Propagation, July 1967.

The scattered vector potential at the surface of the thin wire antenna satisfies the following differential equation

$$\left(\frac{\partial^2}{\partial z^2} + \beta^2\right) A_z(a, z) = -j \frac{\beta^2}{\omega} E_z^{inc}, \quad (A1)$$

where the assumed but suppressed time dependence is $\exp(j\omega t)$, β is free-space propagation constant, ω is the radian frequency, $A_z(a, z)$ is the vector potential at point z and E_z^{inc} is the incident electric field. The solution of (A1) is

$$A_z(a, z) = C_1 \cos \beta z - j \frac{\beta}{\omega} U, \quad (A2)$$

where $U = \beta^{-1} E_z^{inc}$ and C_1 is an arbitrary constant. Another representation for the vector potential is

$$A_z(a, z) = \frac{\mu_0}{4\pi} \sum_{n=-\infty}^{\infty} \int_{\alpha_n}^{\gamma_n} dz' I_n(z') K(z, z'), \quad (A3)$$

where $I_n(z')$ is the current on the n th antenna,

$$\alpha_n = (2n - 1)h + 2n\delta, \quad (A4)$$

$$\gamma_n = (2n + 1)h + 2n\delta, \quad (A5)$$

$$K(z, z') = \frac{\exp \left[-j\beta \sqrt{(z - z')^2 + a^2} \right]}{\sqrt{(z - z')^2 + a^2}}. \quad (A6)$$

Because of symmetry the current distributions on all the antennas are identical, i.e.,

$$I_n(z') = I_0[z' - 2n(h + \delta)]. \quad (A7)$$

Using (A7) and a simple change of integration variable in (A3) yields

$$A_z(a, z) = \frac{\mu_0}{4\pi} \sum_{n=-\infty}^{\infty} \int_{-h}^h du I(u) \cdot K[z, u + 2n(h + \delta)] , \quad (A8)$$

where the zero subscript of the current distribution is deleted for simplicity of notation. Combining (A2) and (A8)

$$\begin{aligned} & \int_{-h}^h du I(u) \bar{K}(z, u) \\ &= \frac{4\pi}{\mu_0} C_1 \cos \beta z - j \frac{4\pi U}{\zeta_0} , \end{aligned} \quad (A9)$$

where

$$\bar{K}(z, u) = \sum_{n=-\infty}^{\infty} K[z, u + 2n(h + \delta)] .$$

The constant C_1 may be determined by requiring the current go to zero at the end of the antenna. Of course, this is not the proper boundary condition when the ends of the antenna are so close to the plates that this end current is no longer negligible.

For convenience, define C_1' such that—

$$C_1' = \frac{4\pi}{\mu_0} C_1 . \quad (A10)$$

The numerical solution of (A9) is obtained by approximating the integration with a finite sum at N different points (method of moments). The resulting linear algebraic equations are

$$\begin{aligned} \sum_{m=1}^N I(Z_m) \Pi_{mp} &= \Gamma_p \\ p &= 1, 2, 3, \dots, N . \end{aligned} \quad (A11)$$

$$\Pi_{mp} = \int_{(m-1)\Delta}^{m\Delta} du \left[\bar{K}(z_p, u) + \bar{K}(z_p, -u) \right], \quad (A12)$$

$$\Gamma_p = C_1' \cos \beta z_p - j \frac{4\pi}{\zeta_0} U. \quad (A13)$$

By simple algebraic manipulation

$$\Pi_{mp} = g(p - m) + g(p + m - 1), \quad (A14)$$

$$g(m) = \int_0^{\Delta} dv \sum_{n=-\infty}^{\infty} K[m\Delta, v + 2n(h + \delta)] \quad (A15)$$

where

$$\left. \begin{aligned} z_m &= (m - 1)\Delta \\ z_p &= (p - 1)\Delta \\ \Delta &= h/N \end{aligned} \right\}. \quad (A16)$$

The aforementioned boundary condition requires

$$I(z_N) = 0, \quad (A17)$$

which should apply when $\delta > a$. Using (A17) in (A11) yields the system of equations

$$\sum_{m=1}^{N-1} I(z_m) \Pi_{mp} - C_1' \cos \beta z_p = -j \frac{4\pi}{\zeta_0} U, \quad (A18)$$

$$p = 1, 2, \dots, N,$$

which has N unknowns and N equations.

In Figure A2, the center current of the receiving antenna between parallel plates is shown as a function of frequency and plate separation. It shows a relatively small dependence upon plate separation except in the region of resonance. Here it is observed that the presence of the plates tends to diminish the amplitude of the current without changing the resonant frequency. Figure A3 exhibits the change in the distribution of current for changes in plate separation.

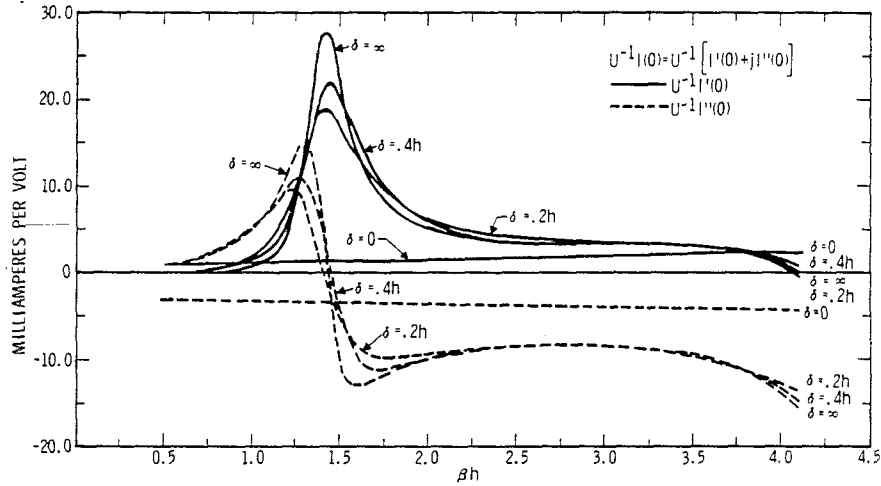


Figure A-2. Center current as a function of electrical length for various plate separations, $\Omega = 2Pn(2h/a) = 10$.

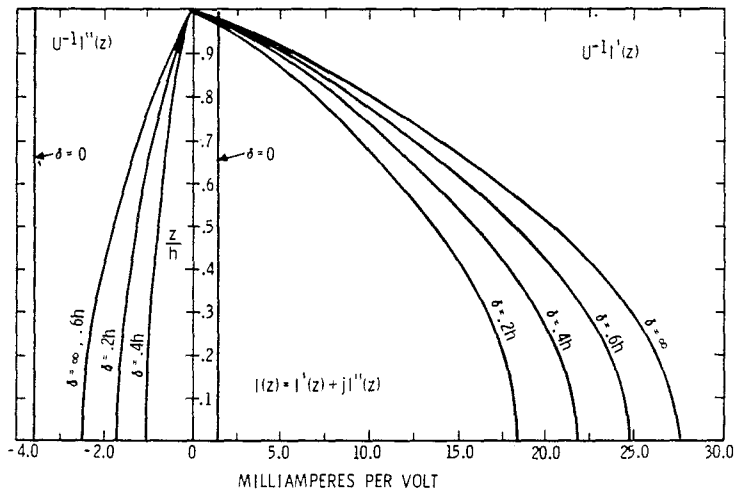


Figure A-3. Current distributions for various plate separations. $\beta h = 1.45$, $\Omega = 2Pn(2h/a) = 10$. Note that the left and right abscissa scales are different.